Neutron Penumbral Imaging : 1. A Quantitative Evaluation on Isoplanaticity of Toroidal-Segment Aperture

Neutron Penumbral Imaging : I. A Quantitative Evaluation on Isoplanaticity of Toroidal-Segment Aperture

Yen-Wei CHEN and Zensho NAKAO

Abstract

A quantitative study is made on performance of neutron penumbral imaging with a toroidal-segment aperture, and it focused on isoplanaticity of aperture point spread function and effect of the non-isoplanaticity on the reconstructed images. The results show that the aperture point spread function is satisfactorily isoplanatic for a small field of view, while for a large field of view the point spread function is not satisfactorily isoplanatic resulting in some distortion in the reconstructed image and reduction of resolution.

Key words: penumbral imaging, neutron image, toroidal aperture, point spread function isoplanatic, non-isoplanaticity, field of view, spatial resolution

1. Introduction

In laser fusion research, the implosion symmetry is one of the most important issues in achieving high-density compression. To date, the symmetry of a compressed core has been diagnosed using x-ray, α-particle[1], [2] and proton [3] imaging techniques. In recent laser fusion experiments, compression of fusion fuel to densities in the range of several hundred times the liquid density has been achieved [4], so that x-rays, α-particles and protons are re-absorbed within the compressed core. Therefore, new diagnostic methods are necessary to image highly penetrating neutrons.

The major difficulty in implementing a neutron imaging system is the penetration of the neutrons through a material used to make the imaging aperture. Penumbral imaging, one of coded aperture imaging techniques, is proposed for imaging of such very penetrating radiations by Nugent et al. [5], [6]. The technique uses the facts that spatial information can be recovered from the shadow or penumbra that an unknown source casts of simple large circular aperture. Since such an aperture can be "drilled" through a substrate of almost any thickness, the technique can be easily applied to very penetrating radiations such as neutrons and γrays. The penumbral imaging technique has been successfully used to laser fusion experiments for neutron imaging at Lawrence Livermore National Laboratory [7] and ILE, Osaka University [8].

The performance of penumbral imaging has been studied in detail by computer simulations [9], [10]. The studies included the influence of various factors such as grain noise, statistical errors, and uncertainties in the camera geometry. For effective imaging of neutrons, the aperture must be thick enough to block 14-MeV neutrons in order to provide sufficient image contrast. Thicker is the aperture, lower is the isoplanaticity of the aperture point spread function (PSF) [11]. Since the penumbral imaging is based on a linear deconvolution technique [5], the non-isoplanaticity will introduce a significant distortion in the reconstructed image. The isoplanaticity of the aperture PSF is also an important issue for neutron imaging.

In the developed neutron penumbral imaging system [7], [8] a toroidal-segment was proposed and used as an aperture taper in order to provide a sharp and isoplanatic PSF. Though the toroidal-segment aperture has the advantage of good isoplanaticity compared to other conventional aperture[7], [8], [11], there are no detail studies on the PSF isoplanaticity of the toroidal-segment aperture. The purpose of this paper is to make a quantitative evaluation on the PSF isoplanaticity of the toroidal-segment aperture and the effect of the non-isoplanaticity on the reconstructed image. A quantitative analysis is done for the developed neutron penumbral imaging system.

2. Penumbral imaging

The basic concept of the penumbral imaging technique is shown in Fig.1. Penumbral imaging is a two-step technique. The first step is encoded image formation. A source of incoherent radiation casts a geometrical shadow through a large circular aperture to produce the encoded image that consists of a uniformly bright region surrounded by a penumbra (*hatched* region). Information about the source is encoded in this penumbra. The second step is reconstruction or deconvolution

Received: 20 May, 1996
Department of Electrical and Electronic Engineering, Faculty of Engineering

of the encoded image to determine the shape of the original source using numerical techniques.

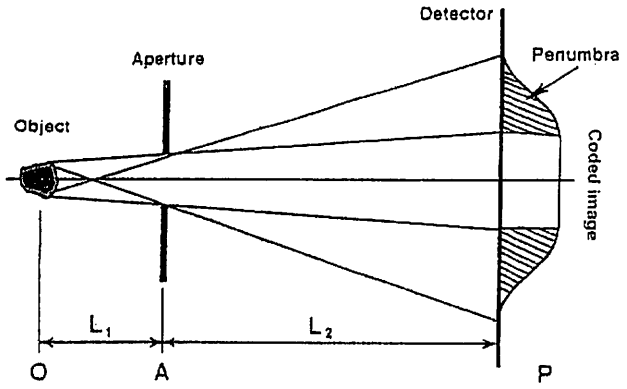

Fig. 1 The basic concept of penumbral imaging.

It is easy to show that the encoded image $P(\mathbf{r})$ is given by [12]

$$P(\mathbf{r}) = \int A(\mathbf{r};\mathbf{r}')\cdot O(\mathbf{r}')\,d\mathbf{r}' ; \qquad (1)$$

where $A(\mathbf{r})$ is the point spread function (PSF) of aperture, $O(\mathbf{r})$ is the function describing the source.

If the PSF of the aperture is isoplanatic (space-invariant), the penumbral image can be written as a convolution of the source function (O) and the PSF (A) as [12]

$$P(\mathbf{r}) = \int A(\mathbf{r}-\mathbf{r}')\cdot O(\mathbf{r}')\,d\mathbf{r}' = A * O \qquad (2)$$

where * denotes convolution. Thus given $P(\mathbf{r})$ and $A(\mathbf{r})$, the source function $O(\mathbf{r})$ can be reconstructed by a simple linear deconvolution technique.

In general, deconvolution techniques are very sensitive to noise in the encoded image, because the noise will be amplified to very high levels at spatial frequency region where Fourier amplitude of the PSF is close to zero. We used a parametric Wiener filter [12] for reconstruction of the penumbral image. The Wiener filter $M(\mathbf{u})$ defined in the Fourier transform domain is given as

$$M(\mathbf{u}) = \frac{1}{A_F(\mathbf{u})}\cdot\left(1+\gamma\frac{\sigma^2}{|A_F(\mathbf{u})|^2}\right)^{-1} \qquad (3)$$

where $\mathbf{u}$ is the spatial frequency variable, $A_F(\mathbf{u})$ is the Fourier transform of PSF, σ^2 is the average variance of the noise in the encoded image, and γ is a filter coefficient. The optimum value of γ is determined by computer simulations for different σ^2.

Here it should be noted that if the PSF is not isoplanatic, the linear reconstruction according to Eq. (3) will introduce some distortion.

3. Toroidal-segment aperture and its isoplanaticity

For effective imaging of neutrons, the key point is that the aperture must effectively block 14-MeVneutrons; it should also be specially tapered to provide an isoplanatic (space-invariant) point spread function (PSF) with a sharp edge to allow the linear reconstruction. In order to provide sufficient image contrast, the aperture used in our neutron penumbral imaging system [8] was made from a tungsten (W) block with a thickness (T) of 6cm (the mean free path of 14-MeV neutrons in W is about 3cm), and in order to provide a satisfactorily sharp and isoplanatic PSF, we chose a toroidal-segment for aperture taper as shown in Fig.2. The principle of the toroidal-segment for aperture taper is that the edges of the aperture PSF for different source-points (on or off axis) are sharp and similar as shown in Fig.2(a). The detailed aperture shape and size developed for 14-MeV neutron imaging in ILE, Osaka University is shown in Fig.2(b). The aperture design was based on the neutron source size and required resolution [8]. The larger is the aperture radius of curvature, the sharper is he PSF edge but the less is the field of view.

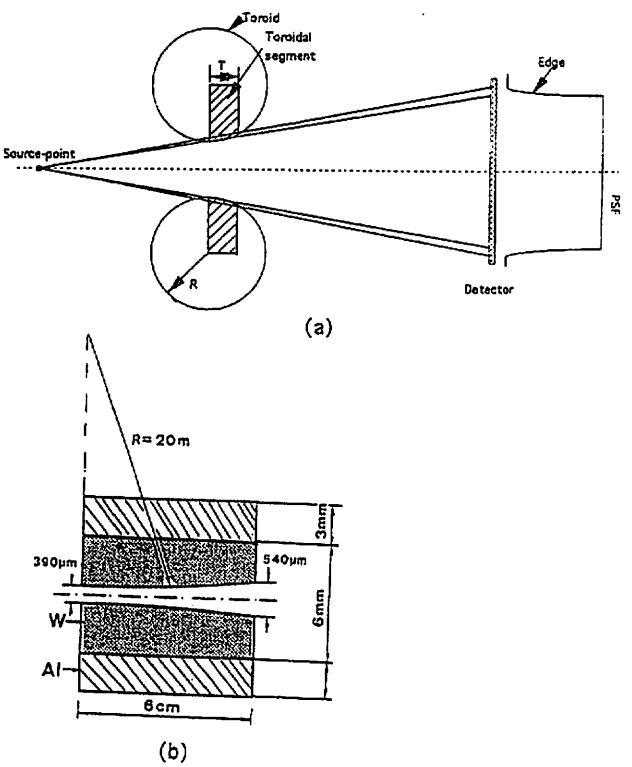

Fig.2 (a) Principle of the toroidal-segment for aperture taper.
(b) Aperture shape and size used in the neutron penumbral imaging system[8]

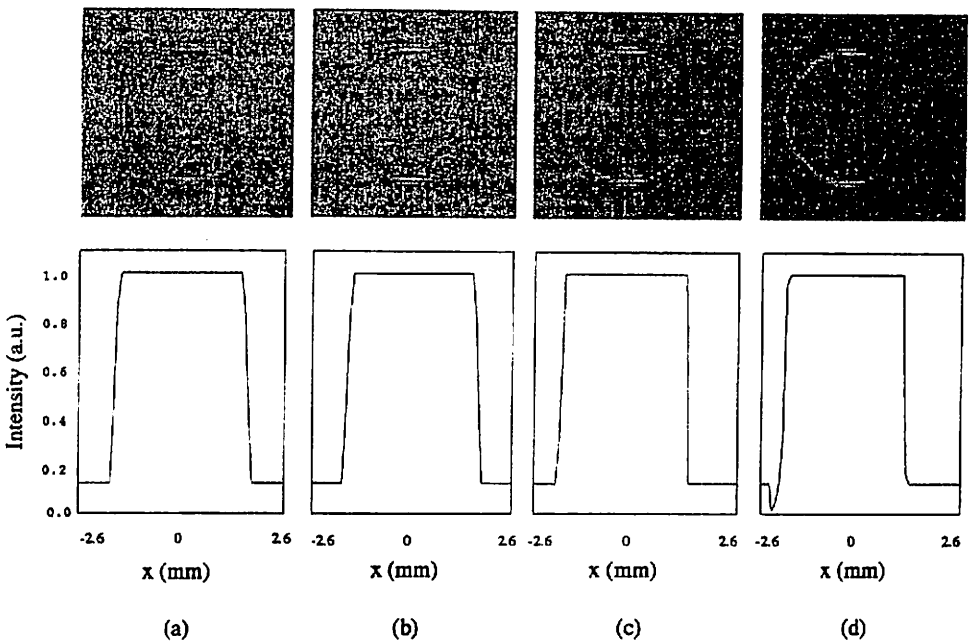

Fig. 3 Point spread functions of toroidal-segment aperture for different displaced source-point. (a) : $\Delta x=0$, (b) : 25 μm, (c) : $\Delta x=50\,\mu$m, (d) : $\Delta x=75\,\mu$m,

Though the toroidal-segment aperture has the advantage of good isoplanaticity, some distortion will be still introduced because the PSF is not perfect isoplanatic. We focused our studies here on the quantitative evaluation of the isoplanaticity of the toroidal-segment aperture and the effect of the non-isoplanaticity on the reconstructed image by computer simulations.

In our computer simulations, as a representative example the developed neutron penumbral imaging system [8] in ILE, Osaka University is used for quantitative analysis because it has been used for imaging of 14-MeV neutrons in real laser fusion experiments. The aperture shape and size are the same as that shown in Fig.2(b). The aperture-to-detector distance (L_2) is 10 times the source-to-aperture distance (L_1). The pixel size or resolution of the detector is 200 μm corresponding to pixel resolution of $\sim$20 μm on the source plane, which is the same pixel resolution with the developed neutron penumbral imaging system used in the laser fusion experiments [8] ($L_2=100L_1$, pixel sizeof detector = 2000 μm). The source-to-aperture distance L_1 is a variable parameter.

The penumbral image (encoded image) is simulated by detailed ray tracing through the aperture, and the radiation is assumed to be exponentially attenuated with a mean free path of 3cm. In addition to the non-isoplanaticity, there are the following three factors which will significantly affect the PSF. One is the neutrons scattered from aperture and chamber, second is the noise due to the statistical uncertainty and third is the alignment error of the aperture. The effects of neutron scattering have been studied using a Monte-Carlo neutron transport code MCNP [13]). The calculation results show that the neutrons scattered from the aperture and chamber can be almost perfectly suppressed by operating a gate system($\sim$25ns) on the detector together using a paraffin shield[8]. So the neutron scattering is not included in the simulations. The noise and the distortion due to the alignment error of the aperture are also not considered here, but they will be discussed in the next section. The reconstruction is done by the Wiener filter as shown in Eq.(3).

Firstly, we show the simulation results for $L_1=12$ cm ($L_1/T=2$). The PSF isoplanaticity of the aperture was studied by detailed ray tracing of a source-point through the aperture. The pixel size of the calculated penumbral image on the detector plane is 200 μm, corresponding to the pixel resolution of 20 μm in the source plane. Figure 3 shows the calculated PSFs for different displaced source-point. In the calculation results, there are about 12% fraction of the neutrons passing directly through the 6cm-thick tungsten substrate caused a uniform background outside the image area, which can be easily removed from the signal by substraction. The images shown in Fig.3 are those after substraction. As shown in Fig.3, it is clear that the difference between the off-axis PSF ($\Delta x>0$) and the on-axis PSF ($\Delta x=0$) increases as the displacement (Δx) increases, which means that the isoplanaticity is decreased as the displacement is increased.

The distortion of resolution for the displaced source-point was estimated by deconvolving the off-axis PSF with on-axis PSF. The calculated effective resolution, which is defined as FWHM of the reconstructed image taken parallel to the displacement, is shown in Fig.4 as a function of the displacement of the source-point from the optical axis. It can be seen that the degradation of the spatial resolution due to the non-isoplanaticity over a field of view (FOV) of 100 μm (displacement of 50 μm) is substantially small compared to pixel resolution (20 μm), while the distortion is significant for a large field of view.

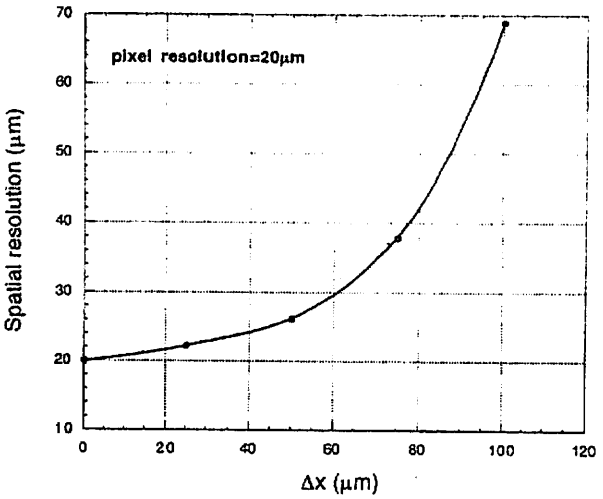

Fig. 4 Spatial resolution of the toroidal-segment aperture as a function of the displacement of the source-point from the optical axis in the source plane.

The effect of non-isoplanaticity on the reconstructed image has also been studied. Figure 5 shows the source-object with a variable size used in simulations. The simulation results for three different object size are shown in Fig.6. Figures 6(a), 6(b) and 6(c) are the penumbral images obtained by detailed ray tracing of the source-object through the aperture. The reconstructed images are shown in Figs.6(a′), 6(b′) and 6(c′),respectively, which are obtained by deconvolving the penumbral image with the on-axis PSF ($\Delta x=0$). It can be seen that there are no significant distortions for the small object (smaller than 100 μm), while there are significant distortions in the reconstructed images for the large object because of the non-isoplanaticity.

Since the isoplanaticity of the aperture PSF is mainly determined by the ratio of source-aperture distance (L_1) to aperture thickness (T), the distortion due to the non-isoplanaticity as shown in Fig.6 can be decreased by increasing the source-aperture distance (L_1). Figure 7 shows the simulation results for $L_1=24$cm

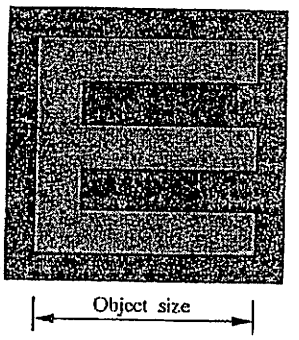

Fig. 5 Phantom with variable size used in simulations.

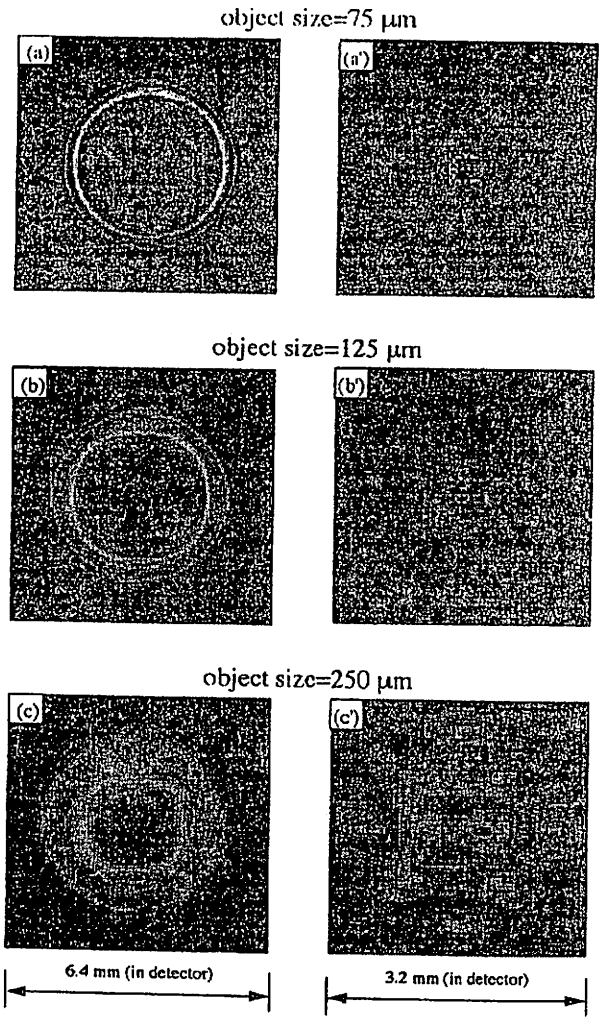

Fig. 6 Simulation results for $L_1=12$cm (L_1/T). (a),(a′):Penumbral image and reconstruction of the object with a size of 75 μm. (b),(b′): Penumbral image and reconstruction of the object with a size of 125 μm. (c),(c′):Penumbral image and reconstruction of the object with a size of 250 μm.

($L_1/T=4$). The improvement of the reconstructed image is evident. There are no significant distortions in the reconstructed images even for the large object.

The dependance of the spatial resolution (FWHM) on the source-aperture distance (L_1) is shown is Fig.8 for a 100μm field of view (solid line) and a 200μm field of view (dashed line)

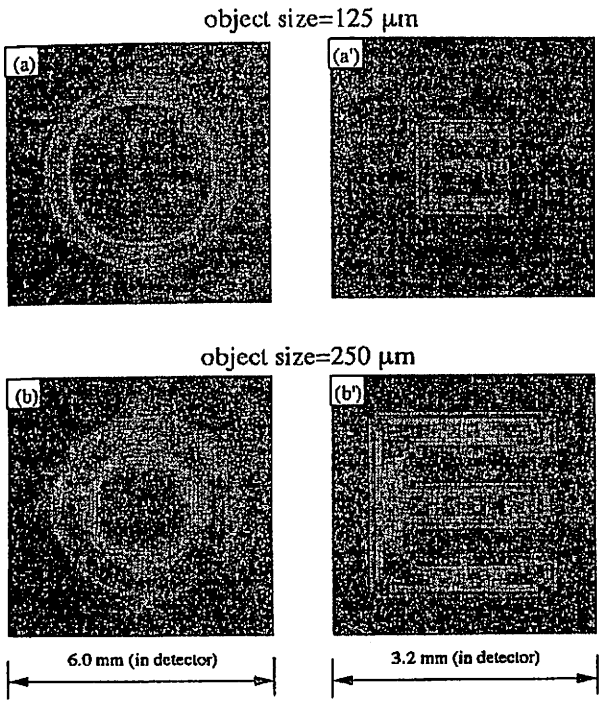

Fig. 7 Simulation results for L_1=24cm (L_1/T=4). (a),(a'):Penumbral image and reconstruction of the object with a size of 125μm. (b),(b'): Penumbral image and reconstruction of the object with a size of 250μm.

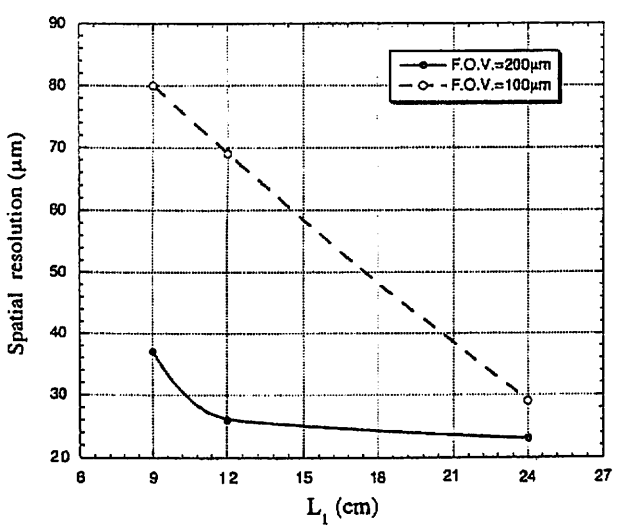

Fig. 8 Spatial resolution as a function of the source-aperture distance (L_1).

4. Discussion and optimization

As we showed in the previous section, the isoplanaticity of the aperture PSF may be improved by increasing the source-aperture distance (L_1). On the other hand, the signal-to-noise ratio (SNR) in each detector element will be $\sqrt{N}$, where N is the number of counts in a single detector element. Since N is proportional to $1/L_1^2$, we see that the SNR in each detector element will be inversely proportional to L_1. The variation of SNR on L_1 for a neutron yield of 5×10^{11} is shownin Fig.9, which is estimated based on the experimental result[8](L_1=12cm) measured by using 14-MeV neutron source OKTAVIAN at Osaka University. The larger is the source-aperture distance, the better is the PSF isoplanaticity, but the lower is the SN ratio. The determination of the source-aperture distance (L_1) is a process of compromise.

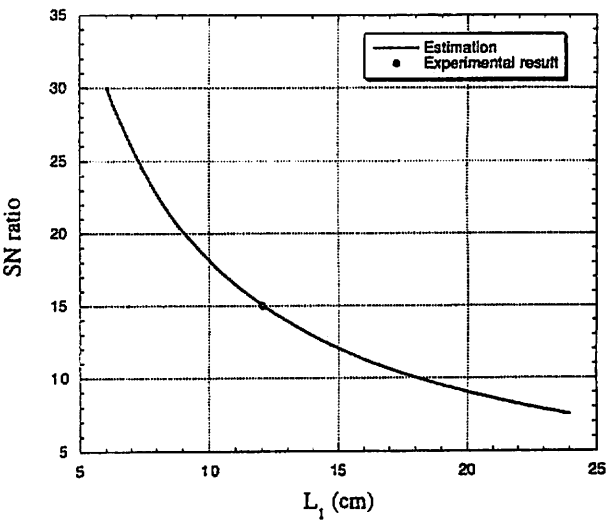

Fig. 9 Variation of the SNR for the neutron penumbral imaging system as a function of the source-aperture distance (L_1).

In order to make a quantitative evaluation, we also simulated the effect of the noise on the resolution. The simulations were performed in the same manner as the previous section with a source-point. We added a Poisson noise to the penumbral image. The SN ratio of the penumbral image used in the simulations is inversely proportional to L_1 as shown in Fig.9. Firstly we show the dependance of the spatial resolution on the SN ratio of the penumbral image in Fig.10. The source-point is assumed on-axis (Δx=0) and the effect of non-isoplanaticity is excluded. It can be seen that the poor SN ratio of the penumbral image will cause a significant reduction of the spatial resolution of the reconstructed image. The spatial resolution including the effect of non-isoplanaticity is shown in Fig. 11 as a function of L_1. The solid line is the resolution of the 100μm field of view and the dashed line is the resolution of the 200μm field of view. It can be seen that for a small source-object(smaller than 100

μm) the best quality image with a resolution of 36 μm can be obtained at L_1=12cm or L_1/T=2, while for a large source-object (larger than 200 μm) the source-aperture distance L_1 must be larger than 24cm or $L_1/T \geqq 4$ to obtain the reconstruction with a resolution about 44 μm. The optimum source-aperture distance is determined by the size of neutron source and neutron yield. For recent laser fusion experiments, since the typical burn region (neutron source) size is about 100 μm, the optimum L_1 is about 12cm for the neutron yield (Ny) of 5×10^{11}.

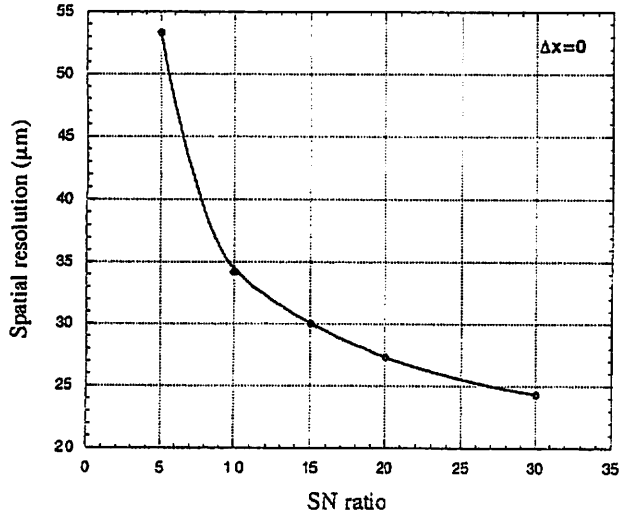

Fig. 10 The effect of noise on the spatial resolyution of the neutron penumbral image.

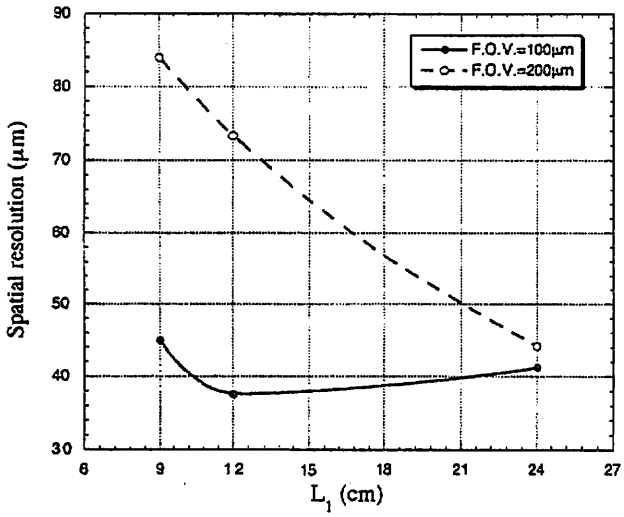

Fig. 11 The spatial resolution as a function of the source-aperture distance (L_1), taking into account the effects of the noise.

Finally, lets consider the distortion due to the aperture alignment error. In our previous work [8], we have shown that the axis of the aperture can be aligned to the optical axis with an accuracy of 240 μrad corresponding to a displacement of ΔX=28 μm (L_1=12cm) in the source plane by using a Moire technique [14]. As shown in Fig.4, the distortion due to the displacement of 28 μm is substantially small compared to the pixel resolution of 20 μm.

5. Summary

Using computer simulations, we have studied the isoplanaticity of the toroidal-segment aperture and the effect of the non-isoplanaticity on the spatial resolution and reconstructed images. The results show that the isoplanaticity of the aperture PSF depend on the source size, source-aperture distance. The isoplantaticity is degraded as increasing the field of view.Though the isoplanaticity can be improved by increasing the source-aperture distance but in the cost of reduction of SN ratio. The spatial resolution of the developed neutron penumbral imaging[8] has been quantitatively estimated as 36 μm for a field of view of 100 μm and 44 μm for a field of view of 200 μm, taking into account the effect of noise due to the statistic uncertainty (Ny=5×10^{11}) and pixel resolution (20 μm).The pixel resolution can be easily minimized by using a larger magnification of the camera and the detector with a smaller element size (detector resolution). A new nonlinear reconstruction method based on a genetic algorithm has also been developed for reconstruction of neutron images with a larger field of view [15].

Acknowledgements

The authors would like to express their thanks to Profs. M.Yamanaka and N.Miyanaga of the Institute of Laser Engineering, Osaka University for their helpful advice throughout the study. They also want to thank Mr. K.Arakaki for his support on computer calculations.

References:

[1] N.M.Ceglio and L.W.Coleman, "Spatially resolved α emission from laser fusion targets", Phys. Rev. Lett., Vol.39, No.1, pp.20-24 (1977).

[2] Y.-W.Chen, N.Miyanaga, M.Yamanaka, H.Azechi, K.Nishihara, T.Yamanaka, S.Nakai and C.Yamanaka, "Observation of burn and pusher regions of laser-driven larger-high-aspect-ratio target by α-particle imaging", *Jpn. J. Appl. Phys.*, Vol. 29, No.10, pp.2135-2138 (1990).

[3] Y.-W.Chen, N.Miyanaga, M.Yamanaka, H.Azechi,

S.Ishikawa, T.Yamanaka, S.Nakai and S.Tamura, "Measurement of D D burn region using proton penumbral coded aperture imaging", *Opt. Commun.*, Vol.73, No.5, pp.337-341 (1989).

[4] S.Nakai, K.Mima, T.Yamanaka, Y.Izawa, Y.Kato, K.Nishimura,T.Sasaki,M.Nakatsuka,M.Yamanaka, H.Azechi, T.Jitsuno, T.Norimatsu, K.A.Tanaka, N.Miyanaga, M.Nakai, M.Takagi, Y.-W.Chen, H. Katayama, R.Kodama, H.Nakaishi, Y.Setsuhara, A.Nishiguchi, T.Kanabe and C.Yamanaka, "Six hundred times solid density compression of directly driven hollow shell pellets", *Plasma Physics and Controlled Nuclear Fusion Research*, Vol.3, pp.29-39 (1990).

[5] K.A. Nugent and B.Luther-Davies, "Penumbral imaging of high-energy x-rays from laser-produced plasmas", *Opt. Commun.*, Vol.49, No.6, pp.393-396, Apr. 1984.

[6] K.A. Nugent and B.Luther-Davies, "Application of penumbral imaging to thermonuclear neutrons", *J. Appl. Phys. Vol.58*, No.7, pp.2508-2515 (1985).

[7] D.Ress, R.A. Lerche, R.J.Ellis, S.M.Lane and K.A.Nugent, "Neutron imaging of laser fusion targets", *Science*, Vol.241, No.4868, pp.956-958 (1988).

D.Ress, R.A. Lerche, R.J.Ellis, S.M.Lane and K.A.Nugent, "Neutron imaging of inertial confinement fusion targets at Nova", *Rev. Sci. Instrum.*, Vol.59, No.8, pp.1694-1696 (1988).

[8] Y.-W.Chen, N.Miyanaga, M.Unemototo, M.Yamanaka, T.Yamanaka, S.Nakai, T.Iguchi, M.Nakazawa, T.Iida and S.Tamura, "High resolution penumbral imaging of 14-MeV neutrons", *IEICE Trans. on Electronics*, Vol.E78-C, No.12, pp.1787-1792 (1995).

[9] K.A. Nugent and B.Luther-Davies, "Potential and limitations of penumbral imaging", *Appl. Opt.*, Vol.25, No.6, pp.1008-1014 (1986).

[10] Y.-W.Chen, Ph.D dissertation, Osaka University, (1990).

[11] D.Ress, "Design of thick aperture for high -resolution neutron penumbral imaging", *Proc. of IEEE Nuclear Science Symposium*, pp.1-5 (1989).

[12] A. Rosenfeld and A.C. Kak, *Digital Picture Processing*, 2nd Edition, Academic Press, New York, (1982.)

[13] LASL Transport Group X-6, LA-7396-M, (1981).

[14] D.Ress, "Neutron penumbral imaging of laser-fusion targets", *Energy and Technology Review*, LLNL, (1988).

[15] Y.-W.Chen, Z.Nakao and K.Arakaki, "Neutron penumbral imaging: II. Distortion-free reconstruction by genetic algorithms", *Bulletin of the Faculty of Engineering, University of the Ryukyus*, No.52, pp.165-170 (1996).